COMPUTATION METHODS FOR SPACE HARMONIC EFFECTS ON SINGLE-PHASE INDUCTION MOTOR PERFORMANCE

VALENTIN NĂVRĂPESCU[1], MIRCEA POPESCU[2], AUREL-IONUȚ CHIRILĂ[1], IOAN-DRAGOȘ DEACONU [1], CONSTANTIN GHIȚĂ[1]

Key words: Single-phase induction motors, MMF harmonics.

Single-phase and two-phase induction machines are widely used in commercial applications. The developed methods for the analysis of the single-phase induction motor, *i.e.* forward-backward field, symmetrical components and cross-field methods, can be adapted for modelling the MMF harmonic effects. This paper presents a review on all these methods that demonstrates the equivalence between models and shows how the equivalent circuit elements can be interchanged from one method to another.

1. INTRODUCTION

Single-phase and two-phase induction machines are widely used in commercial applications due to their cost and high reliability. Significant performance deterioration of the systems driven by single or two-phase induction machines may appear due to winding harmonics that create parasitic torques at all speeds, typically causing "dips" in the torque/speed characteristic. Core and rotor copper losses are also increased due to the MMF harmonic effects and thus the motor efficiency is diminished. Both odd and even harmonic effects have been considered using the double revolving field theory [1–2]. The other developed methods for the analysis of the single-phase induction motor, *i.e.* symmetrical components and cross-field methods, can be adapted for modelling the MMF harmonic effects. The following assumptions are made: 1. The stator windings are built with half-cycle symmetry and consequently only the odd MMF harmonics are considered; 2. All the MMF harmonics experience the same level of saturation; 3. The rotor current is treated as a current sheet that varies as a true harmonic function with respect to the position around the air-gap; 4. The effect of skewing is ignored.

[1] "Politehnica" University of Bucharest, Sp. Independenței, 313, Sector 6, Bucharest, Romania, E-mail: valentin.navrapescu@plc.pub.ro
[2] University of Glasgow, University Avenue, Glasgow G12 8QQ, United Kingdom

Rev. Roum. Sci. Techn. – Électrotechn. et Énerg., **55**, *3*, p. 278–288, Bucarest, 2010

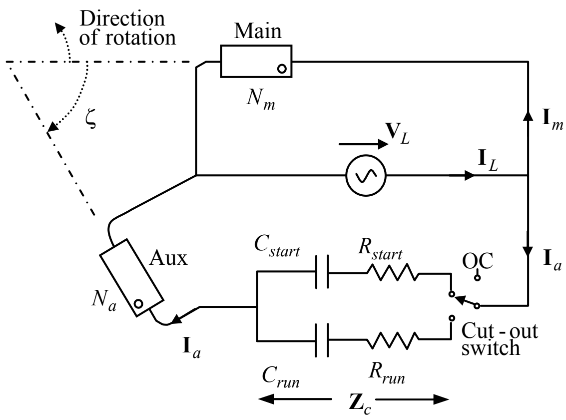

Fig. 1 – Equivalent circuit of the single-phase induction motor connections.

Fig. 1 shows a general equivalent circuit of the single-phase induction motor connections. Experimental torque/speed curves were obtained for two capacitor-run motors, with various main and auxiliary winding distributions. Comparisons between the theoretical and experimental curves show reasonable agreement, with sufficient correlation to provide important guidance on the overall effect of the winding harmonics. The speed of calculation is important because of the large number of possible cases requiring analysis and interpretation, justifying the development of an analytical method in preference to a finite-element approach that may be more time consuming.

2. THEORY

2.1. FORWARD AND BACKWARD REVOLVING FIELD METHOD

The forward- and backward-revolving field method is generally attributed to Morrill [1]. The approach described here is essentially a summary of the lucid account given by Veinott [2], with the addition of the iron loss W_{Fe} that is represented in the equivalent circuit by R_c. The variables are expressed as phasors. Fig. 2 shows the revolving field method applied to a single-phase induction motor when capacitive impedance is in series with the auxiliary winding. The permeance variation caused by the slot openings is neglected. The space harmonics are of odd order and rotate at subsynchronous speeds in both the forward and reverse directions. The impedances presented to the positive-sequence and negative-sequence harmonic MMF distributions are approximated using the following relations:

$$\mathbf{Z}_{fn} = \frac{0.5}{\dfrac{1}{\mathrm{j}X_{mn}} + \dfrac{1+n(1-s)}{R_{rn} + \mathrm{j}\left[1+n(1-s)\right]X_{lrn}}};$$
$$\mathbf{Z}_{bn} = \frac{0.5}{\dfrac{1}{\mathrm{j}X_{mn}} + \dfrac{1-n(1-s)}{R_{rn} + \mathrm{j}\left[1-n(1-s)\right]X_{lrn}}}. \tag{1}$$

The magnetization reactance and the rotor leakage reactance for the n-th harmonic order MMF may be approximated as a function of the reactances corresponding to the fundamental spatial MMF. So, we can use the approximation

$$X_{mn} = \left(\frac{k_{wn}}{k_{w1}}\right)^2 \frac{X_m}{n^2};\ X_{lrn} = \left(\frac{k_{wn}}{k_{w1}}\right)^2 X_{lr};\ R_{rn} = R_{bar}\left(\frac{k_{wn}}{k_{w1}}\right)^2 + \frac{R_{endring}}{n^2}. \tag{2}$$

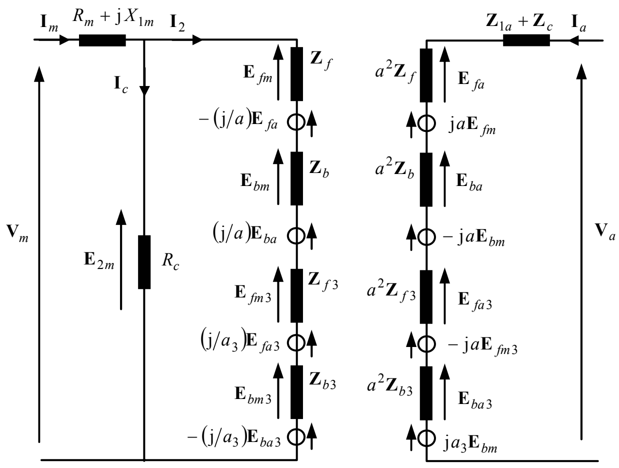

Fig. 2 – Equivalent circuit of 1-phase induction motor with capacitor connection using the forward and backward field theory.

The bar resistance and the end-ring resistance are computed taking into account the skin-effect and the temperature effect [16]. The effective turns ratio that determines the n-th MMF harmonic interaction is:

$$a_n = \frac{T_{ph\,aux}}{T_{ph\,main}} \cdot \frac{k_{wn\,aux}}{k_{wn}}. \tag{3}$$

The harmonic field of order $n = (4k–1)$ will determine a rotation in the opposite sense with the fundamental, while the harmonic field of order $n = (4k+1)$ rotates in the same sense with the fundamental flux wave. The space MMF harmonic effects are more important at low speed and will diminish the starting torque. The resultant torque is computed as:

$$T_e = \frac{P}{2}\frac{1}{\omega_s}\left[\left(T_f - T_b\right) + \ldots + \left(T_{fn} - T_{bn}\right)\right], \tag{4}$$

where the torque produced by the fundamental field is given by:

$$T_1 = \frac{P}{2}\frac{1}{\omega_s}\left(T_f - T_b\right);\ T_f = \mathrm{Re}\left(\mathbf{Z}_f\right)\left|\mathbf{I}_m - \mathrm{j}a\mathbf{I}_a\right|^2;\ T_b = \mathrm{Re}\left(\boldsymbol{Z}_b\right)\left|\boldsymbol{I}_m + \mathrm{j}a\boldsymbol{I}_a\right|^2. \tag{5}$$

The following relations give the torque produced by the n-th harmonic field:

$$\begin{aligned}
&T_n = \frac{P}{2}\frac{1}{\omega_s}\left(T_{fn} - T_{bn}\right); \qquad T_n = \frac{P}{2}\frac{1}{\omega_s}\left(T_{fn} - T_{bn}\right);\\
&T_{fn} = n\,\mathrm{Re}\left(\boldsymbol{Z}_{fn}\right)\left|\boldsymbol{I}_m + \mathrm{j}a_n\boldsymbol{I}_a\right|^2;\ T_{fn} = n\,\mathrm{Re}\left(\boldsymbol{Z}_{fn}\right)\left|\boldsymbol{I}_m - \mathrm{j}a_n\boldsymbol{I}_a\right|^2;\\
&T_{bn} = n\,\mathrm{Re}\left(\boldsymbol{Z}_{bn}\right)\left|\boldsymbol{I}_m - \mathrm{j}a_n\boldsymbol{I}_a\right|^2;\ T_{bn} = n\,\mathrm{Re}\left(\boldsymbol{Z}_{bn}\right)\left|\boldsymbol{I}_m + \mathrm{j}a_n\boldsymbol{I}_a\right|^2;
\end{aligned} \tag{6}$$

$$n = 4k + 1, \quad n = 4k - 1.$$

2.2. SYMMETRICAL COMPONENTS METHOD

Fig. 3.a shows the symmetrical-component model where only the fundamental and the 3rd MMF harmonic are illustrated. The model for the fundamental MMF was originally described by Veinott [2] and Suhr [3].

By association with the forward-backward field method, the positive sequence corresponds to the forward rotating field and the negative sequence to the backward rotating field. With fixed values for the iron-loss resistors, the currents can be calculated explicitly, and in this case the computational burden is not greatly increased by including them; but there remains the problem of knowing what values to use. The approach described here relies on two elements not available to the original authors: one is the extremely fast solution by computer, and the other is the ability to estimate the iron loss independently from the flux-density waveforms. Indeed it is possible to re-evaluate the iron loss recursively from the flux-density waveforms as the solution proceeds, causing R_{cf} and R_{cb} to vary. However, in the split-phase induction motor there are so many other departures from the ideal model, that this enhancement may make little difference to the overall accuracy. For example, stray loss, inter-bar currents, winding harmonics, and various manufacturing imperfections may have a combined effect that is greater than the iron loss, which is often relatively small in these motors. The values of the resistors R_{cf} and R_{cb} cannot be measured directly, but only roughly correlated with a series of calculations over a range of operating conditions. For this reason it is an advantage to have more than one analytical model, and in the next section a third method is described – the cross-field model – which includes the iron-loss resistors corresponding to the main and auxiliary winding circuits. The impedances presented to the both sequences harmonic MMF distributions are approximated using the following relations:

$$\mathbf{Z}_{fn} = \frac{0.5\alpha_n}{\mathrm{j}X_{mn} + \dfrac{1+n(1-s)}{R_{rn} + \mathrm{j}\left[1+n(1-s)\right]X_{lrn}}};\mathbf{Z}_{bn} = \frac{0.5\alpha_n}{\mathrm{j}X_{mn} + \dfrac{1-n(1-s)}{R_{rn} + \mathrm{j}\left[1-n(1-s)\right]X_{lrn}}}. \quad (7)$$

The magnetization reactance and the rotor leakage reactance for the n-th harmonic order MMF may be approximated with similar relations to forward and backward field method (2). The coefficient α_n is computed as:

$$\alpha_n = 0.5\left[1 + \left(\frac{k_{wnaux}k_{w1}}{k_{w1aux}k_{wn}}\right)^2\right]. \quad (8)$$

The coefficient α_n is introduced to take into account the fact that n-th MMF harmonic interaction has different effective turns ratio which is a_n. The transformation from the circuit in Fig. 2 (physical rotating fields) and the circuit from Fig. 3.a (fictitious symmetrical components fields) can be done if the forward and backward impedances from the auxiliary winding are expressed using the same effective turns ratio a. Thus, it would seem necessary to multiply the n-th harmonic impedances with the ratio $(a_n/a)^2$. On the other hand this multiplication would change the harmonic impedance value that is used in the main winding circuit. A possible solution is to use an averaging factor α_n, which will apply to both forward and backward components of the n-th space harmonic impedance. A comparison between equivalent circuits in Figs. 2 and 3a shows that if $a = a_n$ then the rotating forward and backward fields method and symmetrical components method will predict identical results as $\alpha_n = 1$ for this particular case. If k_{wn} or k_{wnaux} are smaller than 0.02, it is practically to set $\alpha_n = 0$. The resultant torque is computed as:

$$T_e = \frac{P}{2}\frac{1}{\omega_s}\left[\left(T_f - T_b\right) \pm \ldots \pm \left(T_{fn} - T_{bn}\right)\right], \quad (9)$$

where the relations give the torque produced by the n-th harmonic field:

$$T_n = \frac{P}{2}\frac{1}{\omega_s}\left(T_{fn} - T_{bn}\right);\ T_{fn} = 2n\,\mathrm{Re}\left(\mathbf{Z}_{fn}\right)\left|\mathbf{I}_f\right|^2;\ T_{bn} = 2n\,\mathrm{Re}\left(\mathbf{Z}_{bn}\right)\left|\mathbf{I}_b\right|^2. \tag{10}$$

Note the sign change when including different n-th harmonics order. The harmonics 3, 7, 11, $4k - 1$, determine a reversed rotation sense as compared to the fundamental field, while harmonics 5, 9, 12, $4k + 1$ determine the same rotation sense with the fundamental field.

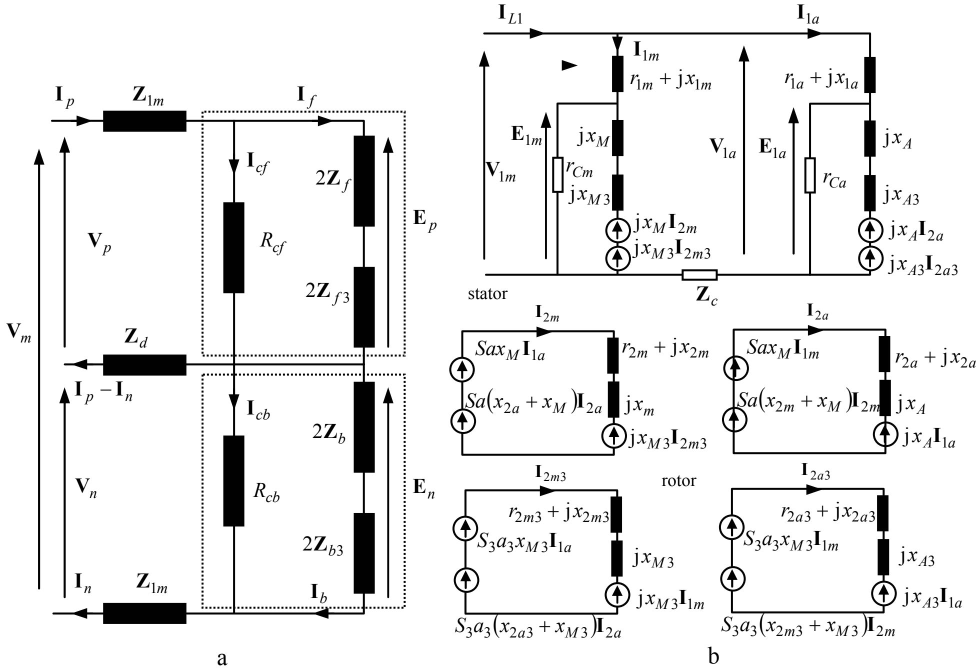

Fig. 3a – Equivalent circuit of 1-phase induction motor with capacitor connection using the symmetrical components theory; b – Equivalent circuit of 1-phase induction motor with capacitor connection using the cross-field theory.

2.3. CROSS-FIELD METHOD

Fig. 3.b shows the cross-field model where only the fundamental and the 3$^{\text{rd}}$ MMF harmonic are illustrated. The model for the fundamental MMF was originally described by Puchstein and Lloyd [4], and Trickey [5]. It assumes a stationary reference frame fixed to the stator and modern theory describes this method as two-axis or dq axis models [12, 15].

This method has a better physical correlation with the actual motor. The main and auxiliary winding circuits are uncoupled and modelled individually, interacting with the entire rotor MMF harmonics. The equivalent iron-loss resistances, r_{Cm} and r_{Ca} are modelled as in [17] with the assumption:

$$r_{Ca} = a^2 r_{Cm}. \tag{11}$$

The per unit speed term that appears in the induced EMFs for the n-th MMF harmonic circuit is:

$$S_n = 1 - [1 + n(1-s)] = n(1-s). \tag{12}$$

The resultant torque is computed as:

$$T_e = \frac{P}{2}\frac{1}{\omega_s}\left(T_1 - T_3 + T_5 - \ldots \pm T_n\right), \tag{13}$$

where the torque produced by the n-th harmonic field is:

$$T_n = a_n \frac{P}{2}\frac{X_{mn}}{\omega_s}\mathrm{Re}\left[\left(\boldsymbol{I}_{1m} - \boldsymbol{I}_{cm}\right)^* \cdot \boldsymbol{I}_{2an} - \left(\boldsymbol{I}_{1a} - \boldsymbol{I}_{ca}\right)^* \cdot \boldsymbol{I}_{2mn}\right], \tag{14}$$

where a_n is computed with (3) and $\mathbf{I}_{cm}$, $\mathbf{I}_{ca}$ represent the currents associated with the core loss in the main winding and auxiliary winding respectively.

The circuit equations shown in Fig. 3.b may be expressed as a matrix system [15], thus any harmonic may be included. The cross-field and forward-backward field methods will produce identical results if the core losses are neglected.

This result is in line with the idea that various locations of the equivalent core-loss resistance in the equivalent circuit do not change the prediction of the overall motor performance. The symmetrical components method is employing an average of the n-th harmonic impedance in the stator windings circuit, and thus will predict identical results with the other two methods only for the case when the stator windings have the same distribution or when the MMF harmonics of the main winding may be neglected.

4. COMPARISON WITH EXPERIMENTAL DATA

All the described methods are validated on three capacitor-run motors with parameters detailed in Table 1. Tested machines were driven according to the standard IEEE 114, as motors using a hysteresis brake and a DC load motor. During the measurements the stator winding and cage rotor temperature are maintained at 40 ^{o}C. In Table 1 the winding factors are presented. The equivalent circuit elements from Figs. 2, 3 are estimated using analytical and numerical methods.

Figs. 4, 5, 6 and 7 show the experimental and computed data.

One should note the for motor 1 while the forward-backward field and the cross-field methods predict almost similar results in agreement with the test data, the symmetrical component method underestimates the torque values between starting and break-down points. The measurements and computations performed for the case from (Fig. 5), show that the symmetrical components method overestimates the 3rd harmonic effect, due to the averaging factor α_n from (8).

This factor would allow a correct model for the space harmonic effects only if the stator windings have a similar distribution or if the main winding has a low harmonics content. For rated load points, all methods lead to results that give good agreement with test data. Motor 2 is an example where the main winding has a very low 3rd harmonic content while the auxiliary winding contains very high 3rd, 5th and 7th MMF harmonics.

Table 1

Winding factors for the tested motors and their parameters up to 7th order

Winding factor	Motor1	Motor2
kw_{1main}	0.8815	0.831
kw_{3main}	0.1944	0.0098
kw_{5main}	0.2540	0.1721
kw_{7main}	0.0442	0.1321
kw_{1aux}	0.9262	0.9577
kw_{3aux}	0.4385	0.6533
kw_{5aux}	0.1021	0.2053
kw_{7aux}	0.2544	0.1576

Motor	# 1	#2
Voltage [V]	220	220
Frequency [Hz]	60	50
Poles	4	2
Capacitor [μF]	40	25
Rated power [W]	1.100	1.000
Rated current [A]	7.1	6.3
Turn ratio *a*	1.097	0.955

Two remark are valid for this case: a) when the main winding's 3rd harmonic from is very low, the auxiliary winding's 3rd harmonic is insignificant for the torque vs speed curve; b) when the values of the main and auxiliary winding factors are similar (k_{wn} / k_{wnaux} about 0.8 ... 1.2) the symmetrical component method predicts similar results with the other two methods even for different windings' distributions.

In connection with the forward-backward field method, a very low winding factor for the n-th harmonic of the main winding eliminates the corresponding harmonic torque regardless of the auxiliary space distribution.

This is an important feature that allows the implementation of an auxiliary winding that maximises the starting capabilities and allows a uniform slot fill factor.

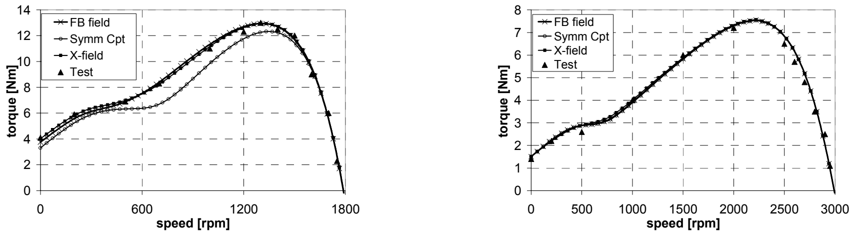

Fig. 4 – Torque *vs.* speed for motor 1 and 2 – energized both stator windings (Table 1).

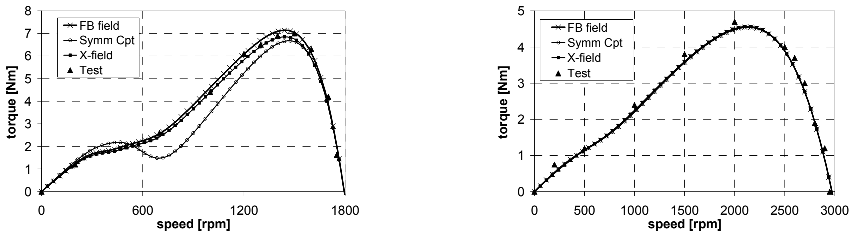

Fig. 5 – Torque *vs.* speed for motor 1 and 2 – energized main winding only (Table 1).

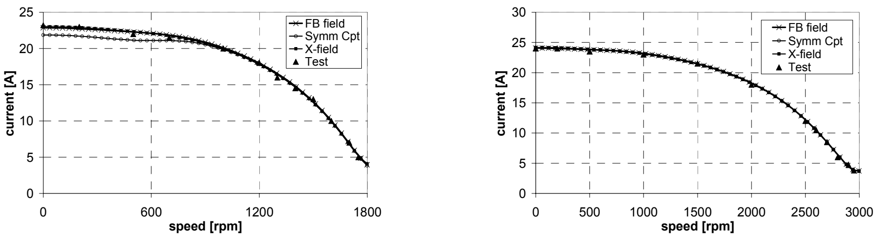

Fig. 6 – Current *vs.* speed for motor 1and 2 – energized both stator windings (Table 1).

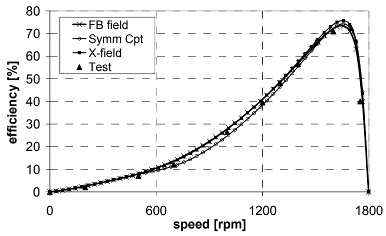

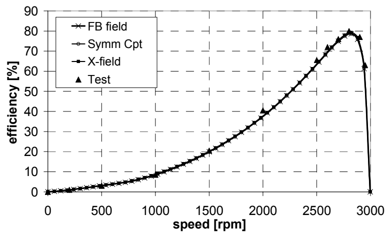

Fig. 7 – Efficiency *vs.* speed for motor 1 and 2 – energized both stator windings (Table 1).

5. CONCLUSIONS

The effects of MMF harmonics in single-phase induction motors can be analytically modelled using any of the three classical methods. The equivalence of the methods is demonstrated in this paper. The forward-backward field and cross field methods may be used for any stator winding distribution and configuration, while the symmetrical components method should be avoided when both windings have an important but different space harmonics content. The core-loss modelling has a minor effect on the accurate prediction of the overall motor performance when equivalent resistances are placed within the equivalent circuits.

Received on 28 November, 2008

REFERENCES

1. W.J. Morrill, *The revolving-field theory of the capacitor motor*, Trans AIEE, April 1929, pp. 614–632.
2. C.G. Veinott, *Theory and design of small induction motors*, McGraw-Hill, New York, 1959.
3. F.W. Suhr, *Symmetrical components as applied to the single-phase induction motor*, Trans. AIEE, **64**, pp. 651–655, September 1945.
4. A.F. Puchstein, T.C. Lloyd, *The cross-field theory of the capacitor motor*, Trans. AIEE, **60**, pp. 58–63, February 1941.
5. P.H. Trickey, *Capacitor motor performance calculations by the cross-field theory*, Trans. AIEE, **76**, pp. 1547–1553, February 1957.
6. L.W. Buchanan, *An equivalent circuit for a single-phase motor having space harmonics in its magnetic field*, IEEE Transactions, PAS-**84**, pp. 999–1007, November 1965.
7. J.H. Davis, D.W. Novotny, *Equivalent circuits for single-phase squirrel-cage induction machines with both odd and even order MMF harmonics*, IEEE PAS-**88**, pp. 1080–1086, July 1969.
8. T.J.E. Miller, *SPEED's Electric Motors*, Magna Physics, ISBN 1-881855-10-4.
9. R.P. Heartz, R.M. Saunders, *Harmonics due to slots in electric machines*, AIEE Trans. (Power Apparatus System), **73**, pp. 946–949, August 1954.

10. H.R. Fudeh, C.M. Ong, *Modeling and analysis of induction machines containing space harmonics*, Part I, II, III, IEEE, PAS-**102**, pp. 2608–2628, August 1983.
11. I. Boldea, T. Dumitrescu, S. Nasar, *Unified analysis of 1-phase AC motors having capacitors in auxiliary windings*, Energy Conversion IEEE Transactions on, **14**, *3*, pp. 577–580, September 1999.
12. P.C. Krause, O. Wasynczuk, S.D. Sudhoff, *Analysis of electric machunery*, IEEE Press, NJ, 1995.
13. P.L. Alger, *Induction machines, their behavior and uses*, Gordon & Breach Science Publishers, New York, London, Paris, Second Edition, 1970.
14. S. Williamson, A.C. Smith, *A unified approach to the analysis of single-phase induction motor*, IEEE Trans. on Ind. Appl., **35**, *4*, pp. 837–843, July-August 1999.
15. M. Popescu, D.M. Ionel, D.G. Dorrell, *Vector control of unsymmetrical two-phase induction motors*, Conf. Rec. IEEE IEMDC 2001, Boston, MA, **1**, pp. 95–101, May 2001.
16. I. Boldea, S.A. Nassar, *The induction machine handbook*, CRC Press, 2001.
17. C.B. Rasmussen, T.J.E. Miller, *Revolving-field polygon technique for performance prediction of single-phase induction motors*, IEEE Trans. on Ind. Appl., **39**, *5*, pp. 1300–1306, Sept.–Oct. 2003.